Use of Cell-Site Diversity in Millimeter-Wave Fixed Cellular Systems to Combat the Effects of Rain Attenuation

Gamantyo Hendrantoro, *Member, IEEE*, Robert J. C. Bultitude, *Senior Member, IEEE*, and David D. Falconer, *Fellow, IEEE*

***Abstract*—An examination of potential advantages of cell-site diversity with selection combining in the context of mm-wave fixed cellular systems is reported. The study involved simulation of converging radio links over weather radar images of the radar reflectivity factor, from which the specific attenuation of rain at 30 GHz was derived. The average correlation of attenuation on two converging links as a function of their angular separation is shown to indicate the potential benefits in the use of cell-site diversity, especially in heavy rain. Results show that diversity gain exhibits a dependence on angular separation θ in the general form of $\sin^k(\theta/2)$. For links of identical lengths the model reduces to a root-sinusoidal shape ($k = 0.5$), whereas links of unequal lengths lead to the ITU-R recommended model ($k = 1$). Based on the $\sin^k(\theta/2)$ model and observation of the length ratio of the links, a set of criteria for determining the benefit of cell-site diversity for a given subscriber location is proposed.**

***Index Terms*—Diversity methods, fixed wireless cellular systems, millimeter wave radio propagation meteorological factors, rain.**

I. Introduction

MOTIVATED by recent interest in North America and Europe in the use of millimeter-wave radio frequencies to provide wireless access to broadband services, embodied in a system generally termed Local Multipoint Distribution System (LMDS), research activities have been initiated worldwide to study the propagation characteristics of millimetric radio waves. One of the natural phenomena that significantly influence the performance of communication systems operating in the cited band, but the study of which has not yet been sufficiently thorough, is rain attenuation. This is particularly true when the influence of rain is put into the context of point-to-multipoint, fixed cellular radio networks, in which spatial statistics of rain attenuation are as important as single-point temporal statistics.

Manuscript received March 12, 2001; revised September 11, 2001. This work was supported by the Canadian Institute for Telecommunications Research in cooperation with the Communications Research Centre. The work of G. Hendrantoro was supported by a Higher Education Project scholarship award from the Indonesian government.

G. Hendrantoro is with the Department of Systems and Computer Engineering, Carleton University, Ottawa, ON K1S 5B6, Canada on leave from the Institut Teknologi Sepuluh Nopember, Surabaya 60111, Indonesia (e-mail: gamantyo@sce.carleton.ca).

R. J. C. Bultitude is with the Communications Research Centre, Ottawa, ON K2H 8S2, Canada (e-mail: robert.bultitude@crc.ca).

D. D. Falconer is with Carleton University, Ottawa, ON K1S 5B6, Canada (e-mail: ddf@sce.carleton.ca).

Publisher Item Identifier S 0733-8716(02)03381-4.

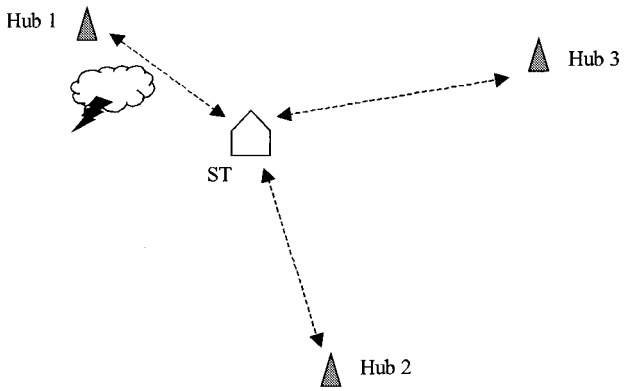

Fig. 1. Typical scenario of cell-site diversity.

At high rainfall intensities, the occurrence of which is of special interest in systems requiring high-reliability links, the horizontal structure of rain is highly variable [1]. It is frequently observed that during a shower, high intensity rain is localized in a very small area surrounded by a region of more uniform, low intensity rain. Hence, in a cellular system under rain with very localized storms, there is a potential that a subscriber terminal receiving a heavily attenuated signal from one hub can obtain less attenuated, acceptable reception from another hub. This makes cell-site diversity appear as a very promising method for improving link reliability and area coverage.

Such a scenario can be roughly sketched as in Fig. 1 for cells with overlapping areas. When the link between a subscriber terminal (ST) and Hub 1, which is the closest and hence the default hub for ST, experiences a performance drop due to a high-intensity shower, there remains a possibility that Hub 2 or 3 can take over the service delivery. Which of the two hubs is selected to receive the handover depends on which hub location results in better signal reception at ST. This is all assuming that the receiver and antenna technology used at the subscriber site allows these links to be monitored simultaneously and continually, and the antenna main beam to be rotated, either electrically or physically, to execute the handover. In principle, it is akin to a macrodiversity scheme employed in mobile cellular systems to combat shadowing effects, taking the advantage of the fact that the effects of obstruction losses around links that connect a mobile terminal to different base stations are only partially correlated [2], [3].

In order to take the spatial variation of rain attenuation into account, field data in the form of radar reflectivity factor

measurements made during rain in the Montreal area were used as the basis for link attenuation calculations. This area is located in rain region D1 according to Crane's model [1] or K according to ITU-R climate maps [4]. Hypothetical links were simulated over the radar measurement area, on each of which the rain attenuation was derived from the radar reflectivity measurements.

The only work similar in scope and methodology was reported by Tan and Pedersen [5] for the European LMDS frequency band around 42 GHz. They used radar images collected over a period of two years, over which they simulated arrangements of diversity systems with two identical-length links and selection combining. Their result suggested a sinusoidal model to predict diversity gain variation with respect to angular separation, which was subsequently adopted in an ITU-R recommendation [6].

The model and results reported here are different from those in [5]. In particular, the gain for two links aligned in approximately opposite directions with respect to the hub was discovered in our study to be relatively insensitive to their angular separation. Thus a separation of, say, 110° between the two branches of a diversity system is adequate to yield a near maximum diversity gain. It was consequently considered that the half-sinusoid model of gain variation with angular separation could be improved by modifying the sinusoidal shape to accommodate for this insensitivity. Our results suggest further that cell-site diversity is potentially advantageous only to subscribers at particular locations, which will be shown later in this paper. In addition, our study considers configurations of links with unequal lengths, a situation that was not studied in [5].

The paper begins with a brief description of the radar measurements and the simulation of radio links on radar images in Section II. Section III examines the correlation function of rain attenuation on converging links as a function of angular separation. An evaluation of diversity gain statistics for a few combinations of link lengths and angular separation is reported in Section IV. Observations regarding these statistics were used as the basis of the empirical model proposed and described in Section V. Finally, a summary is given in the last section.

II. Radar Measurements and Radio Link Simulation

Data analyzed in the work reported herein were recorded by McGill University researchers at the J.S. Marshall Radar Observatory during field measurements of radar reflectivity factors (in mm^6/m^3) over a circular area of 45-km radius centered at Montreal. The S-band horizontally scanning radar system that was used for the measurement is located near the Macdonald campus of McGill University in Montreal. The radar system operates at a wavelength of 10.4 cm with a peak transmit power of 800 kW and a 9.15-m-diameter parabolic dish. It measures the energy scattered back by hydrometeors as well as other objects (clutter) in the coverage area. The recorded data were converted into radar reflectivity factors by McGill University researchers and were subsequently stored and delivered to the authors in the logarithmic form (in dB relative to 1 mm^6/m^3).

The radar measurements were sequentially made for 24 elevation angles, but only those made for an elevation angle of 3.4° were used in this study. At this elevation, the recorded radar image is not overly contaminated by the undesired detection of ground clutter and the snow melting layer. Sufficient data for a circular radar image with a resolution of 1° × 150 m were recorded every five minutes. More details on the radar system and measurements can be found in [7] and [8].

In each radar image element (bin or pixel), a measurement of average radar reflectivity factor Z in mm^6/m^3 was obtained, which corresponds to a specific value of rain intensity (mm/hr) and specific attenuation (dB/km). An estimate of specific attenuation Y in a bin can be obtained from Z by applying:

$$Y = 1.74 \times 10^{-3} Z^{0.776}. \tag{1}$$

The coefficients of the above power–law relationship were derived previously by the principal author from raindrop size distribution measurements made in Montreal and Toronto [7], [9].[1] The values adopted are for vertically polarized radio waves at 30 GHz, 0 °C water temperature, and raindrop shape as given by Oguchi's oblate spheroid model [11].

Two circular regions within the radar coverage area that were free from the effects of ground clutter and the melting layer were selected, within which radial radio links were simulated. The centers of these circular areas are physically located at approximately 17 km SW and 22 km SSW of Montreal, respectively. The radial radio links were separated by 1° from one another. Rain attenuation A (dB) on a simulated link is computed by integrating the estimates of specific attenuation Y (dB/km) along the link. This is calculated for every radial link at various distances from the center, ranging from 1 to 5 km with 100-m resolution, hence allowing simulations and analysis of diversity configurations with different link lengths. An attenuation estimate $A(L, \phi, t)$ is associated with a radial link of length L km and azimuth ϕ with respect to the center, which is simulated on a radar image recorded at time t.

The recording of radar measurements used in the analysis spanned a period of almost two years, commencing in October 1998 and ending in October 2000 with some periods of radar inactivity in between. The total number of usable radar records in the database is 138 939.

III. Angular Correlation

To gain preliminary insight into the potential advantage offered by cell-site diversity, the correlation of attenuations on two converging links was investigated. The correlation measure considered herein is the normalized angular autocorrelation function of rain attenuation (expressed in linear terms) averaged over all simulation samples. For each set of common-ended radial

[1]The determination of these power–law coefficient values was initially motivated by a desire to re-examine the specific attenuation versus rain intensity or radar reflectivity relationships published in the past with the aid of drop size distribution measurements made with modern instruments. These instruments were expected to produce more accurate measurements of the drop size spectrum compared to previous results that resulted in the Marshall–Palmer drop size distribution model [7], [9]. The latter was the basis upon which the ITU-R recommended coefficient values for rain intensity-to-specific attenuation conversion was derived [10]. The study reported in [7] and [9] found slight differences between the newly derived values and those recommended in [10] for frequencies around 20–30 GHz.

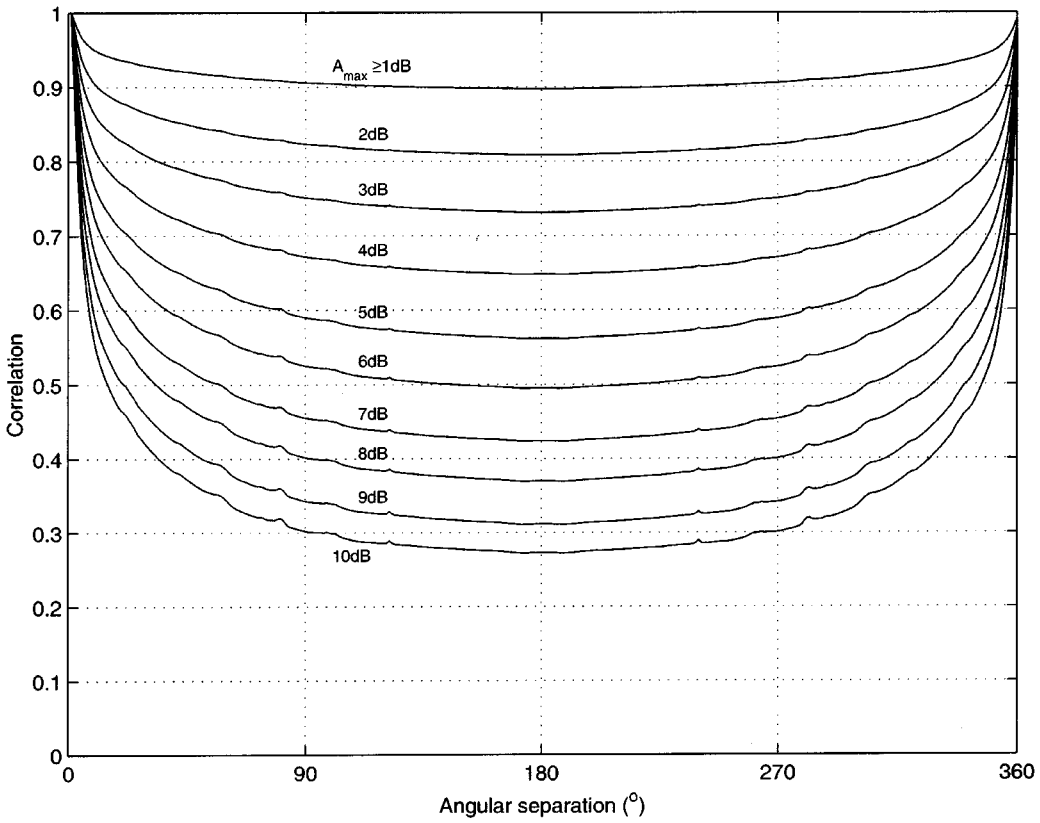

Fig. 2. Average correlation function for two, 2-km-long converging links with different angular separations at the point of convergence.

links simulated on a radar record for time t, the angular autocorrelation $\rho(L, \theta, t)$ between attenuation levels on two links of identical length L kilometers separated in azimuth by θ degrees was evaluated by applying the circular correlation procedure. The results from all simulations were then averaged over the whole radar measurement period. That is

$$\rho(L, \theta) = \left\langle \frac{\sum_{\phi=0^\circ}^{359^\circ} 10^{A(L,\phi,t)/10} 10^{A(L,((\phi+\theta))_{360},t)/10}}{\sum_{\phi=0^\circ}^{359^\circ} \left(10^{A(L,\phi,t)/10}\right)^2} \right\rangle_t \quad (2)$$

where $A(L, \phi, t)$ denotes the rain attenuation in dB on a radial link at azimuth ϕ degrees at measurement time t, $((\bullet))_n$ means that the summation inside the double brackets is done modulo n, and $\langle\bullet\rangle_t$ indicates averaging over time. This function is computed for a specific value of L and is used to examine the variation of correlation in attenuation for different separation angles, regardless of the azimuthal orientation of the paired links.

To study the effect of rain intensity a number of curves of the average correlation function $\rho(L, \theta)$ were computed, each corresponding to a different attenuation (X dB). The correlation function of a set of radial links spanning 360°, whose maximum attenuation is $A_{\max}$, was included in the averaging to obtain the curve associated with attenuation X only if $A_{\max} > X$. The result for two 2-km links is shown in Fig. 2. The ten curves from top to bottom represent the correlation for $X = 1, 2, \ldots, 10$ dB.

Two observations can be made from Fig. 2. Firstly, the magnitude of the correlation decreases when the limit for maximum attenuation is greater. This indicates that correlation of attenuation among different links is less when the radio cell area contains high-intensity rain cells, as anticipated. Secondly, it can be seen that all correlation curves decrease steeply when the separation angle increases from 0° to around 100°, are relatively flat for separation between 100° and 260°, then increase rapidly again toward 360°. This raises an expectation that cell-site diversity would be almost equally effective for all angular separations of the two radio links ranging between 100° and 260°.

IV. Cell-Site Diversity Gain

A. Diversity Gain Computation

Since it is apparent that for a range of angular separations at moderate and high rain rates, correlation of attenuations on two converging links is low, it is considered to be of interest to examine potential diversity gains. Diversity gain is defined herein as the difference in link attenuation in dB for a given percentage of time between single link and diversity configurations. That is, diversity gain $G(p)$ at percentage of time p can be obtained as follows:

$$G(p) = A(p) - A_d(p) \quad (3)$$

where $A(p)$ and $A_d(p)$ are the single-link and two-link attenuations, respectively. For diversity with selection combining, each sample A_d of the two-link attenuation is computed as

$$A_d = \min(A_1, A_2) \quad (4)$$

with A_1 and A_2 being attenuation levels on the two links.

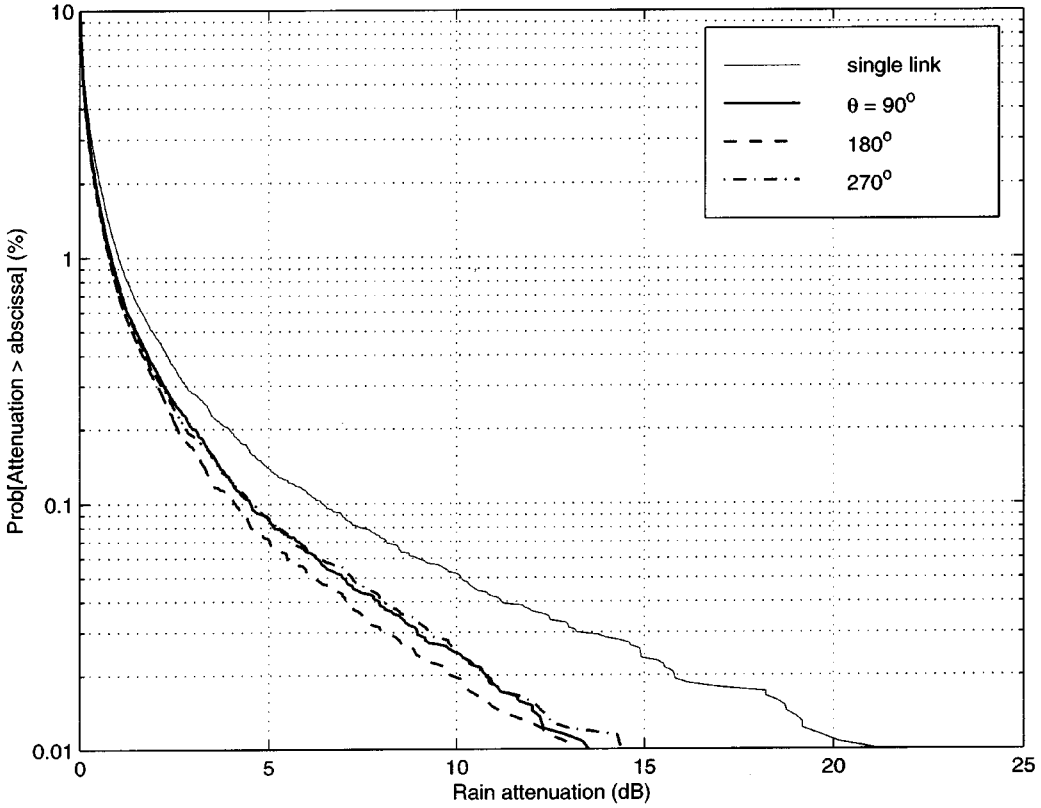

Fig. 3. CCDFs of rain attenuation for single-link and two-branch diversity configurations, in which the link length for both branches is 2 km.

In addition to the adoption of selection combining for this study, it is also assumed that both links of the diversity structure are under LOS conditions at all times and experience clear-sky attenuation that obeys a free-space quadratic increase with range. Otherwise, both links are assumed to be blocked with approximately equal and small shadowing loss. The free-space condition is achieved when an antenna with a very narrow beam in both azimuth and elevation is employed at both ends of the links, such that the effects of multipath propagation can be ignored.

By the above assumptions, for a configuration with two links identical in length, (4) for selection diversity can be applied directly with A_1 and A_2 denoting rain attenuation only on the first and second link, respectively. That is, the link selected at any time is simply the one with the lower rain attenuation. However, for a configuration in which one of the links is shorter than the other, (4) was applied differently. In this case A_1 denotes rain attenuation on the shorter link, while A_2 represents the sum of rain attenuation on the other, longer link and an extra term to account for the difference in free space loss between them. Hence

$$\begin{aligned} A_1 &= A_{1,\,\mathrm{rain}} \\ A_2 &= A_{2,\,\mathrm{rain}} + 20\log(L_2/L_1) \end{aligned} \tag{5}$$

where $A_{n,\,\mathrm{rain}}$ and L_n represent rain attenuation (dB) and length (km) of the nth link, respectively, with the first link being the shorter.

B. Results From Radar Measurements

All available radar images were included in the simulations. Several scenarios were considered for the simulated diversity configurations. Fig. 3 shows complementary cumulative distribution functions (CCDFs) of rain attenuation for cases in which the two diversity branches are both links of 2-km length with separation angles of 90°, 180°, and 270°. Fig. 4 shows the CCDFs for configurations with the same three angular separations, but with the main link 2 km long and the alternate 3 km in length. In this case, the effect of the difference in propagation range is taken into account by applying equation (5). The two results presented here were obtained by setting the 2-km link oriented at an azimuth of 0° with respect to the converging point as the fixed reference.

It can be observed from Fig. 3 that for this particular arrangement, for percentages of time greater than 1% there is little gain offered by the diversity scheme with two 2-km links. However, the diversity gain is greater for smaller time percentages. For two 2-km links with 180° separation, the gain is approximately 2 dB at 0.1% and 5 dB at 0.03%. Thus, diversity serves as protection against rare occurrences of heavy convective rain.

In addition, Fig. 3 shows that for 1% of the time, the difference in the diversity gain for various separation angles is negligible. At 0.1%, the scheme with 180° separation is better by less than one dB compared to the 90° and 270° separations. At 0.03%, this difference becomes approximately one decibel. It, therefore, appears that for this diversity configuration there is not much to be gained when the angular separation is increased

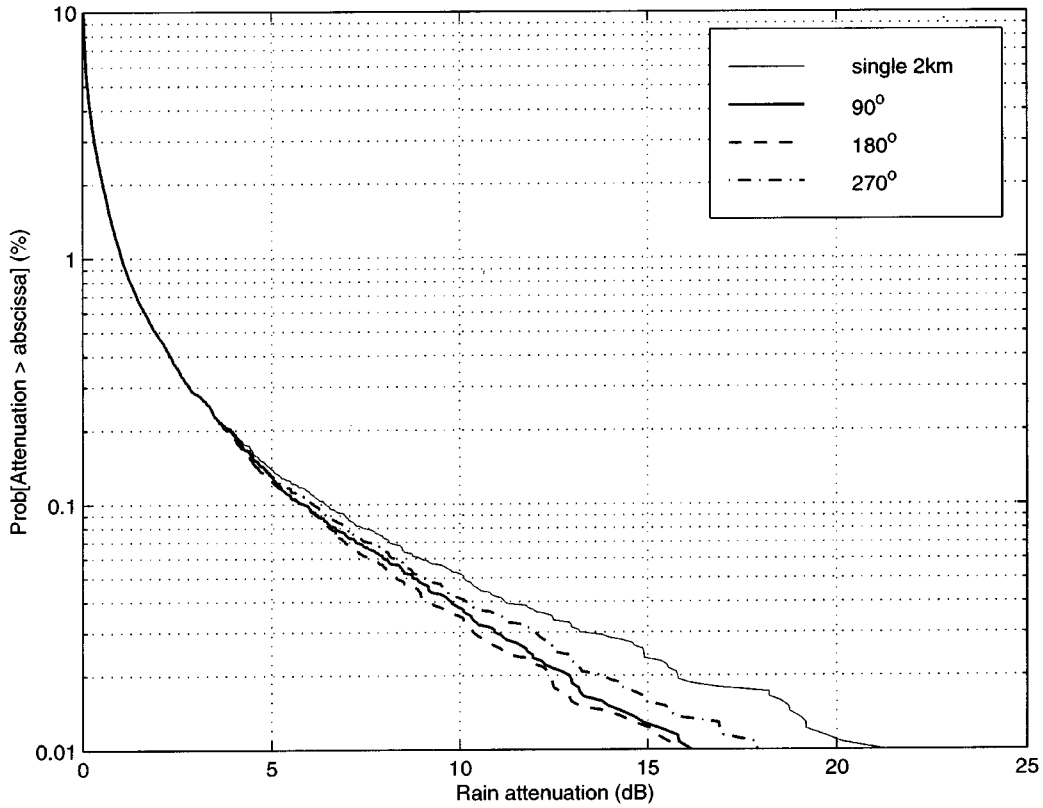

Fig. 4. CCDFs of rain attenuation for single-link and diversity configurations for a main branch and alternative link lengths of 2 and 3 km, respectively.

from 90° to 180°. A general conclusion, however, is presented later in the paper when results from using multiple references at different azimuths are examined statistically.

Diversity gain diminishes when the second link is 3 km in length, as shown in Fig. 4. There is negligible gain at 0.1%, whereas at 0.03% the gain becomes approximately 3 dB for 180° separation. This is ascribed to the difference in path length that leads to the clear-sky path loss on the second link being larger by about 3.5 dB than that on the main link according to (5).

From Fig. 4 for the case of 2- and 3-km links, it is observed that diversity gain for 90° separation is greater than that for 270°, giving an impression of asymmetry in the spatial distribution of rain. However, results for different reference azimuths show different variations of gain with angular separation, which could be caused by the two-year limitation of radar data used in the simulation. The following examination of the average of this function over configurations with reference links pointing at different azimuths shows near-symmetrical variation of diversity gain around 180° separation.

The solid line in Fig. 5 depicts average diversity gain for two 2-km links at 0.1% probability as a function of angular separation computed from multiple simulations with reference links oriented at different azimuths that ranged from 0° to 330° with 30° steps. The figure also shows the range of $\pm\sigma$ around each average gain, where σ is the standard deviation of gain for that particular separation angle. A curve in the form of $G_{180^\circ}\sin^k(\theta/2)$ is given by the dashed line, with parameters G_{180° and k computed by nonlinearly fitting the expression to the simulation results.

It can be observed from the figure that, firstly, the diversity gain shows some amount of variation when cases with different reference azimuths are examined. Asymmetry of the gain around an angular separation of 180° in individual cases is noticeable from the asymmetry of the standard deviation values around 180°. However, the average gain appears to be symmetrical around 180°. Furthermore, the $G_{180^\circ}\sin^k(\theta/2)$ curve fit approximates well the diversity gain average. Based on consideration of these observations, it is concluded that a model to be used in diversity gain prediction should include consideration of results for diversity arrangements with reference links having different azimuthal orientations.

V. Modeling for Prediction of Cell-Site Diversity Gain

A. Considerations

Based on previous sections, the following two guidelines can be established. Any model to be developed should reflect relative flatness in diversity gain for angular separation in the 100°–260° range and should be symmetrical with respect to 180° separation.

The sinusoidal model [5] already takes symmetry into account in predicting diversity gain for a specific angular separation. However, the model shape around its peak at 180° appears too sharp when compared to the shape of the diversity gain variation obtained from radio cell simulations. In addition, the modeling reported in [5] also lacked treatment for diversity configurations with two links having different lengths. It is therefore

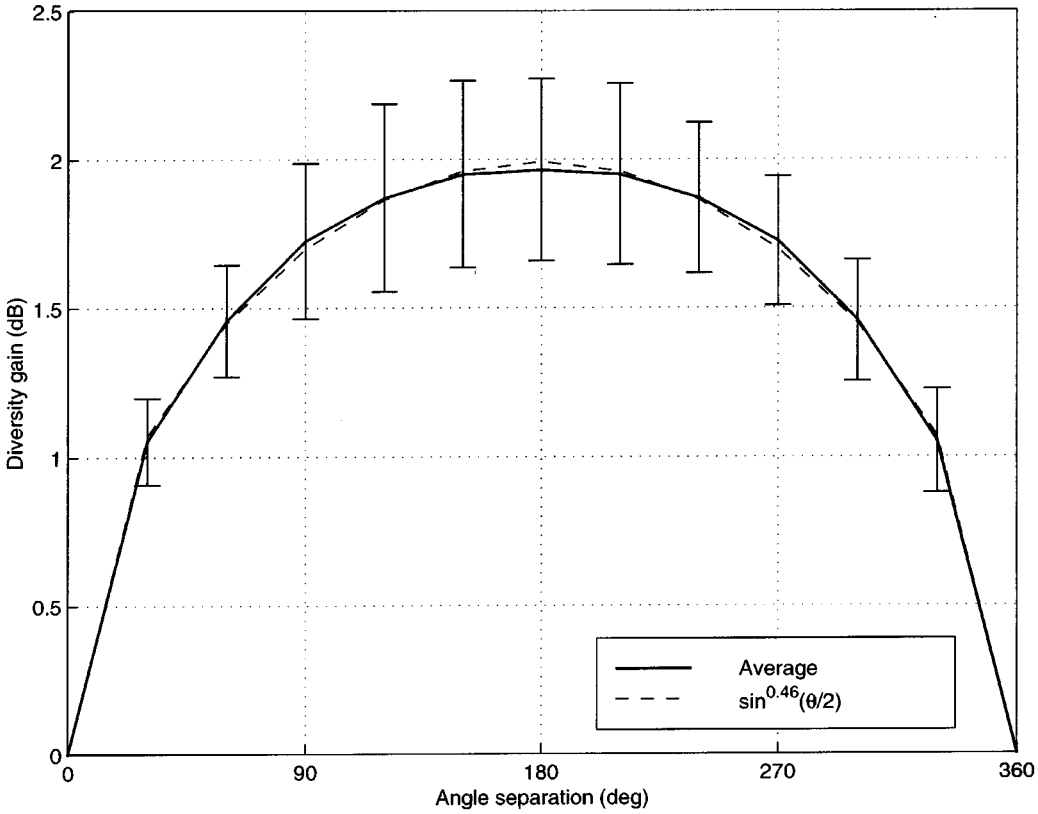

Fig. 5. Diversity gain for 2-km links arrangements.

considered necessary to propose a new model to eliminate these problems.

B. Assumptions and Limitations

It is assumed that the relation describing the variation of diversity gain with angular separation is symmetrical around 180°. On average, diversity gain is maximum when the angle separating the two links is 180°, that is, when the two diversity branches are oriented opposite to one another.

The model proposed is applicable only for LOS links operating at 30 GHz in the rain region into which the area surrounding Montreal has been classified and the range of link lengths used in the simulation study. The range of link lengths considered herein limits the application of this model for cellular systems consisting of small cells only, with typical spacing between adjacent hubs of 2–8 km.

C. Prediction Model

With all the above points being considered, a new model for cell-site diversity gain is proposed in the following form:

$$G(\theta, p) = G_{180^\circ}(p)\sin^{k(p)}(\theta/2), \qquad 0^\circ < \theta < 360^\circ \quad (6)$$

where $G(\theta, p)$ is the diversity gain obtained for angular separation of θ at fading time percentage of p%, $G_{180^\circ}(p)$ and $k(p)$ are parameters of the model that vary for different combinations of link lengths.

This model was fit through nonlinear regression using the Gauss–Newton method [12] to diversity gain values calculated from simulations with the reference links pointing at azimuths that ranged from 0° to 330° with 30° spacing as before. In the case of two links of unequal lengths, the shorter link was taken as the reference, that is, $L_1 \leq L_2$. The fitting procedure produced pairs of parameters G_{180° and k for various combinations of link lengths and percentages of time.

Some of the fitted curves are presented in Figs. 6–9, on each of which the scatter plot of the simulation results and the fitted curves of sinusoid and root sinusoid form are superimposed. These curves are for two diversity scenarios: Figs. 6 and 7 show the results for configurations with both links being of 2 km length, whereas Figs. 8 and 9 exhibit the fit for configurations in which the reference link is 2 km long while the alternative is 3 km. For each scenario, the gain values at fading time percentages of 0.1% and 0.03% (or equivalently, link reliabilities of 99.9% and 99.97%) are shown. A more complete list of the results for length varying between 1 and 4 km and for reliabilities of 99.9%, 99.95%, 99.97%, and 99.99% is shown in Table I. Combinations for which G_{180° yields a value less than 0.5 dB are not shown since such gain levels are considered of little use in practical systems. The two coefficients of the model, G_{180° and k, are given in the table together with their respective confidence intervals at the 95% confidence level [12].

From Figs. 6 and 7 and Table I, it can be observed that for arrangements having two links of equal length $(L_1 = L_2)$, exponent k is in the range of 0.4–0.6. A consistent relation between k and p is not apparent. The values of k are lower for shorter links ($L_1 = L_2 = 1$, 2 km) than for longer ones ($L_1 = L_2 =$

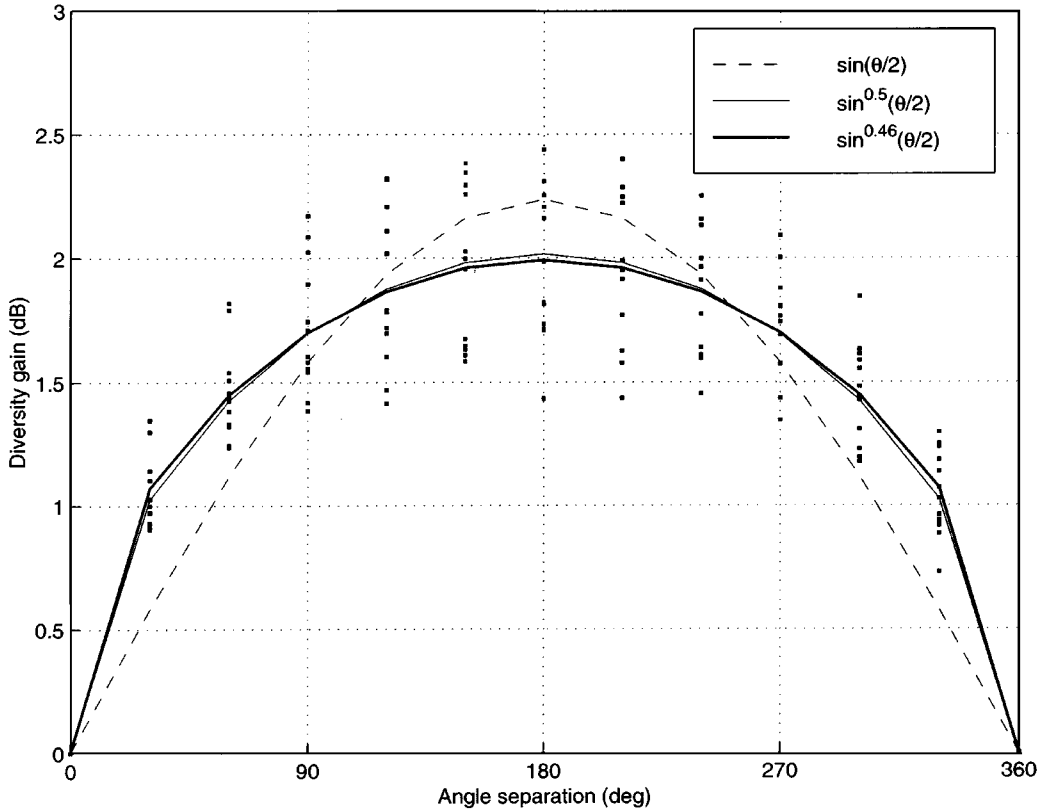

Fig. 6. Diversity gain for two 2-km links at 99.9% reliability.

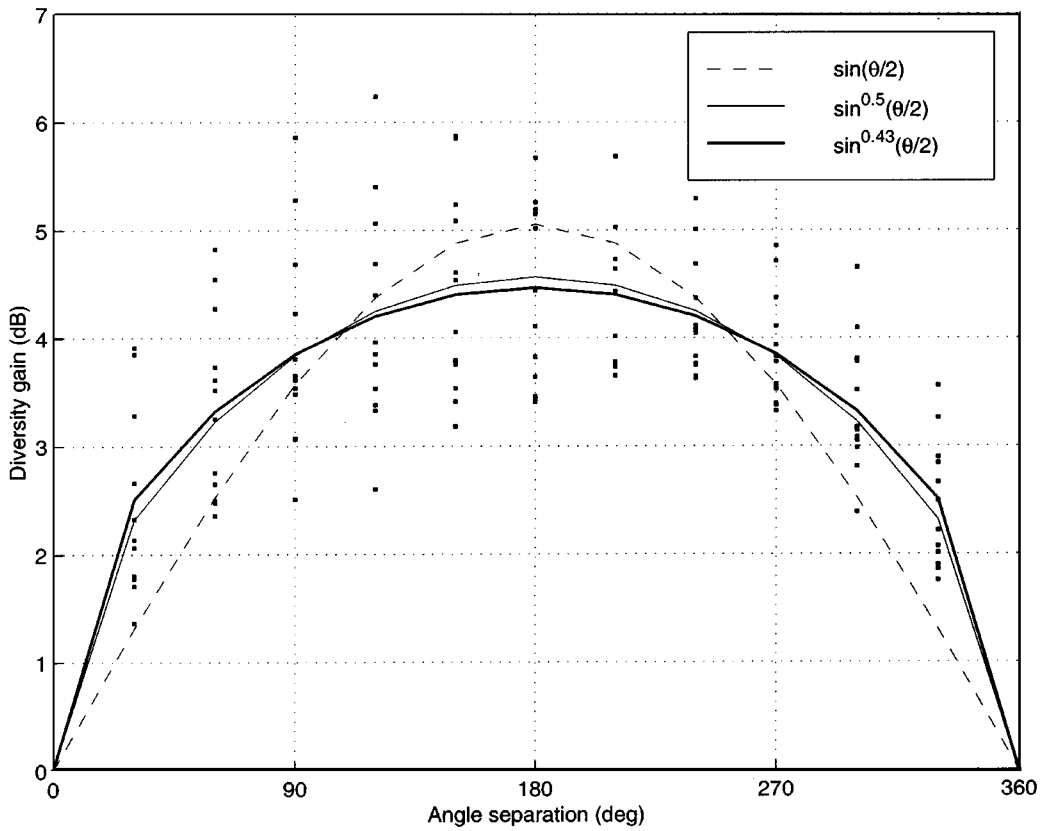

Fig. 7. Diversity gain for two 2-km links at 99.97% reliability.

3, 4 km). For these configurations, the fit to a root-sinusoidal form $G_{180^\circ}\sin^{0.5}(\theta/2)$ produced sums of squared errors only slightly greater than those for the fit to the proposed model with k being optimized through the regression.

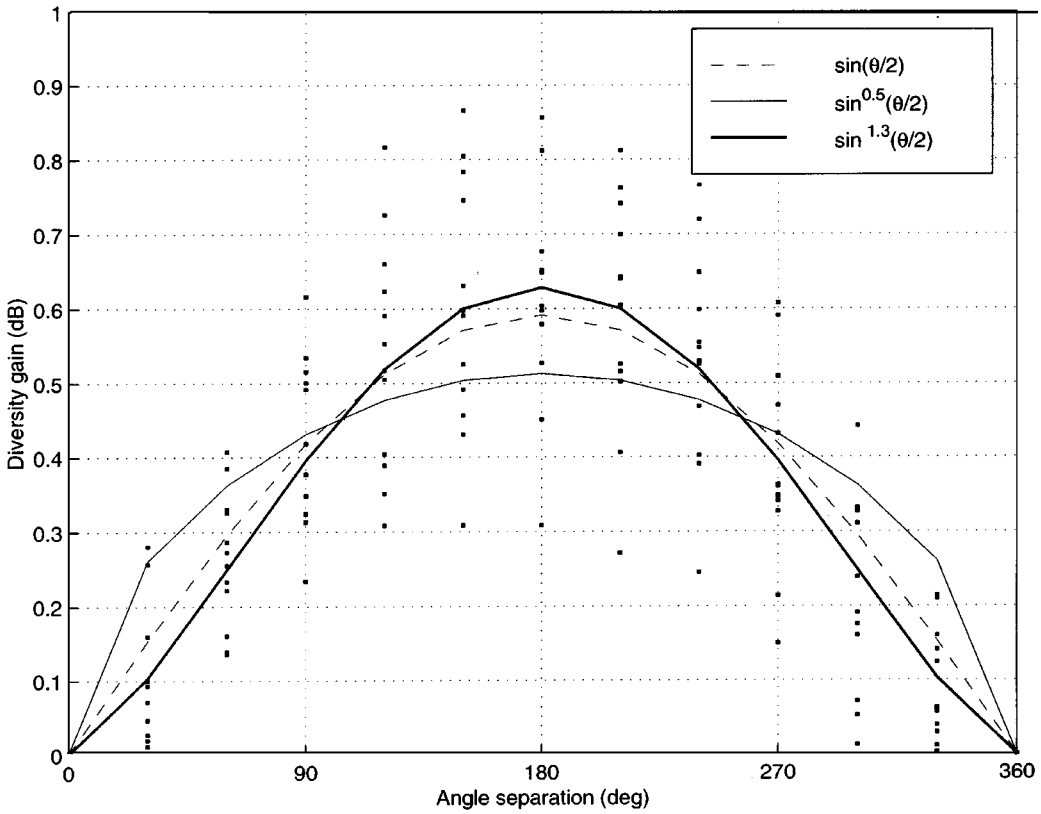

Fig. 8. Diversity gain for 2 and 3-km links at 99.9% reliability.

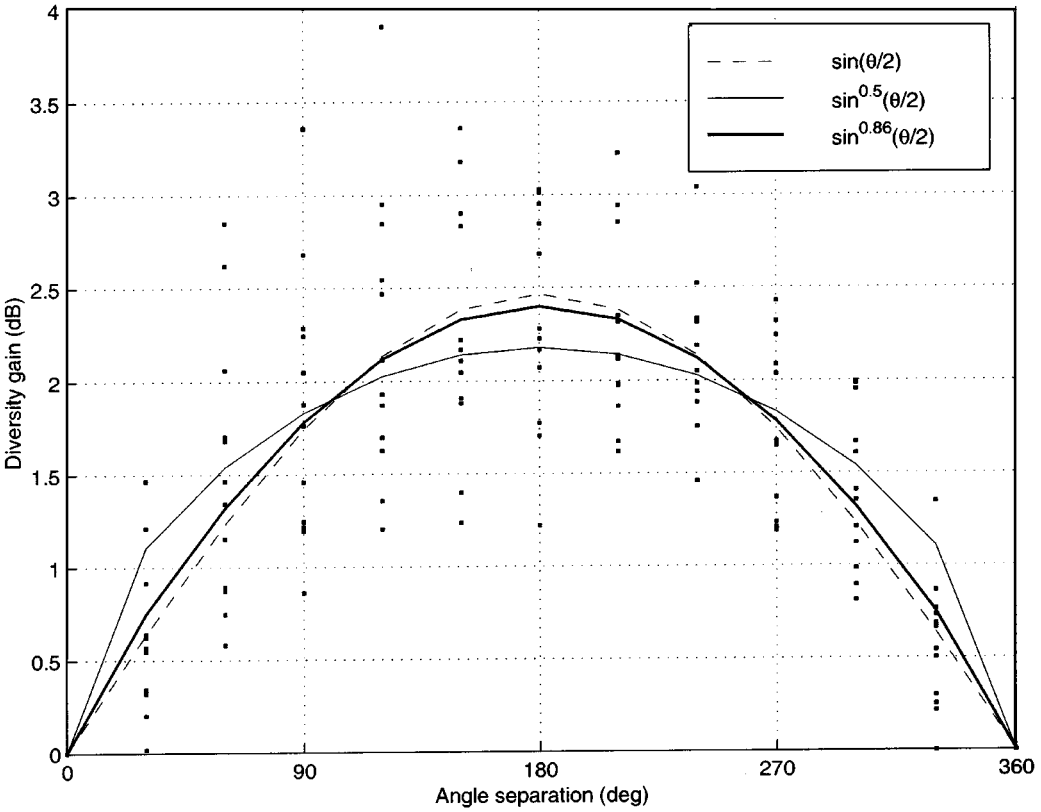

Fig. 9. Diversity gain for 2 and 3-km links at 99.97% reliability.

On the other hand, Figs. 8 and 9 and Table I show that two links of unequal lengths ($L_1 \neq L_2$) yield k values that are approximately in the 0.7–1.4 range, and having a tendency to be lower for higher ratios of L_1/L_2 and higher reliabilities. For these arrangements, the sinusoidal function $(k = 1)$ of angular separation $G_{180^\circ} \sin(\theta/2)$ shows a slightly poorer fit

TABLE I
PARAMETERS OF THE PROPOSED NEW MODEL FOR VARIOUS COMBINATIONS OF LENGTHS AND LINK RELIABILITIES

L_1 (km)	L_2 (km)	Link reliability, 100-p (%)	$G_{180°}$ (dB)	k	Sum of squared errors		
					$\sin^k(\theta/2)$	$\sin^{0.5}(\theta/2)$	$\sin(\theta/2)$
1	1	99.9	0.78 ± 0.03	0.41 ± 0.09	2.3	2.4	4.4
		99.95	1.21 ± 0.08	0.4 ± 0.1	10.8	11.0	16.0
		99.97	1.57 ± 0.09	0.4 ± 0.1	15.7	16.1	25.2
		99.99	3.0 ± 0.2	0.4 ± 0.2	108.4	109.3	138.5
	2	99.99	0.7 ± 0.2	0.7 ± 0.6	42.5	42.7	42.7
2	2	99.9	1.99 ± 0.06	0.46 ± 0.07	7.7	7.7	18.3
		99.95	3.0 ± 0.1	0.43 ± 0.09	33.3	33.9	60.8
		99.97	4.5 ± 0.2	0.43 ± 0.09	75.4	76.9	138.6
		99.99	7.4 ± 0.4	0.5 ± 0.1	263.0	263.8	406.4
	3	99.9	0.63 ± 0.04	1.3 ± 0.2	2.2	3.6	2.3
		99.95	1.31 ± 0.09	1.0 ± 0.2	12.6	15.9	12.6
		99.97	2.4 ± 0.2	0.9 ± 0.2	40.3	46.6	41.0
		99.99	4.4 ± 0.4	0.8 ± 0.2	260.9	276.6	265.8
	4	99.95	0.74 ± 0.08	1.4 ± 0.4	9.2	11.3	9.5
		99.97	1.7 ± 0.1	1.2 ± 0.3	30.5	39.1	31.1
		99.99	3.2 ± 0.4	1.1 ± 0.4	206.1	227.6	206.2
3	3	99.9	3.4 ± 0.1	0.49 ± 0.07	25.6	25.6	52.4
		99.95	5.6 ± 0.2	0.54 ± 0.09	89.6	90.2	144.2
		99.97	7.5 ± 0.2	0.44 ± 0.06	91.1	93.4	254.5
		99.99	13.4 ± 0.7	0.5 ± 0.1	1000.5	1001.4	1439.5
	4	99.9	2.0 ± 0.1	1.0 ± 0.2	20.8	26.7	20.8
		99.95	3.8 ± 0.2	0.9 ± 0.1	60.9	78.0	62.0
		99.97	5.6 ± 0.2	0.8 ± 0.1	81.1	103.9	90.6
		99.99	10.4 ± 0.8	0.7 ± 0.2	1147.6	1180.3	1228.5
4	4	99.9	4.9 ± 0.2	0.47 ± 0.08	66.4	66.6	126.7
		99.95	8.5 ± 0.3	0.49 ± 0.07	147.8	147.8	310.4
		99.97	11.9 ± 0.4	0.53 ± 0.07	231.5	233.2	493.8
		99.99	18.6 ± 0.9	0.5 ± 0.1	1592.2	1601.4	2176.2

compared to the proposed model with k optimized in the regression.

From the examination of the values of $G_{180°}$ in Table I for various combinations of L_1 and L_2, it appears that $L_1/L_2 \geq 0.75$ is necessary to prevent the difference in path loss from dominating over the advantage of diversity. This is true at least at 99.9% reliability and for the range of link lengths considered in the simulation, i.e., 1–4 km. When $L_1 = L_2$, the link length should be at least 2 km in order for $G_{180°}$ to reach 2 dB or more for a reliability of 99.9%, and 3 dB or more for a reliability of 99.95%.

D. Application for Cell-Site Diversity

When using the model given by (6), it is also of interest to determine the range of separation angles for which the decrease in diversity gain from its peak at 180° is expected to be less than a specified percentage δ_g. Equation (6) can be modified to consider this and rewritten as

$$\theta_{\text{cutoff}} = 2\sin^{-1}[(1-\delta_g)^{1/k}] \quad \text{rad}$$
$$= \frac{360}{\pi}\sin^{-1}[(1-\delta_g)^{1/k}] \quad (°) \qquad (7)$$

TABLE II
RANGES OF SEPARATION ANGLES FOR VARIOUS VALUES OF k AND δ_g

k	δ_g		
	5%	10%	20%
0.5	129° - 231°	108° - 252°	80° - 280°
0.7	137° - 223°	119° - 241°	93° - 267°
1.0	144° - 216°	128° - 232°	106° - 254°
1.4	149° - 211°	136° - 224°	117° - 243°

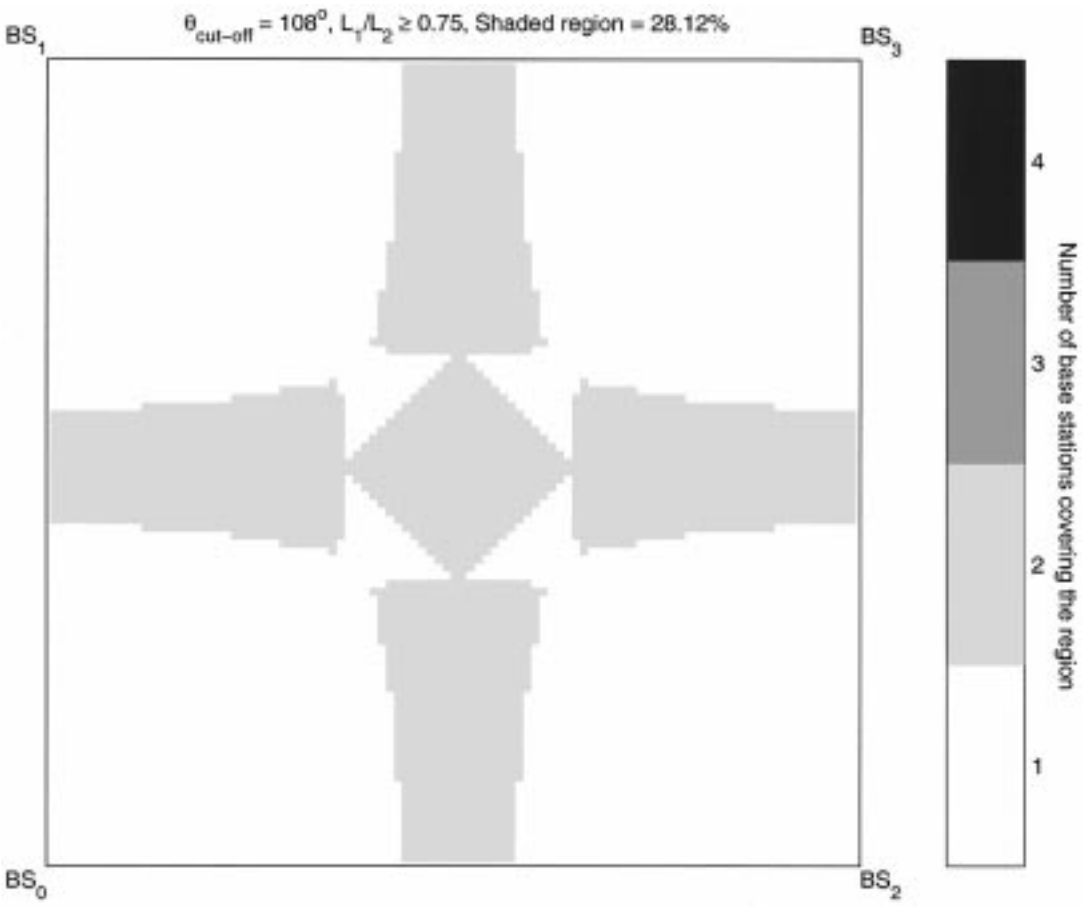

Fig. 10. Areas in a four-sectored rectangular cell that can benefit from cell-site diversity, as predicted by the proposed model with 10% gain reduction allowed.

where θ_{cutoff} is the separation angle for which the diversity gain (dB) diminishes by a portion δ_g from the maximum value at 180°. Although not explicitly stated, the evaluation of the expression also depends on the percentage of outage time or reliability level being considered. Using the case of two 4-km links as an example (see Table I) for which $G_{180^\circ} \approx 5$ dB to attain 0.1% outage time due to rain attenuation, a value $\delta_g = 10\%$ refers to a gain of 4.5 dB for angular separation of θ_{cutoff}. The ranges of separation angles computed using (7) for various values of k and δ_g are given in Table II.

An observation can be made as follows. Consider only diversity systems with links of almost identical length, for which the value of k is approximately 0.5 at any probability level as demonstrated by the results presented in Table I. Also consider that only base stations with angular separations that result in a reduction of 10% or less in diversity gain relative to G_{180° are deemed acceptable. A subscriber located approximately at the same distance from two hubs qualifies as potential user of cell-site diversity when the two hubs and the subscriber subtend an angle in the 108°–252° range.

Based on the foregoing observation, a set of criteria can be proposed to determine whether a subscriber station might benefit from cell-site diversity under rain in a 30-GHz fixed cellular system that employs small cells.

a) The two hubs under consideration must involve links with approximately equal levels of clear sky attenuation to the

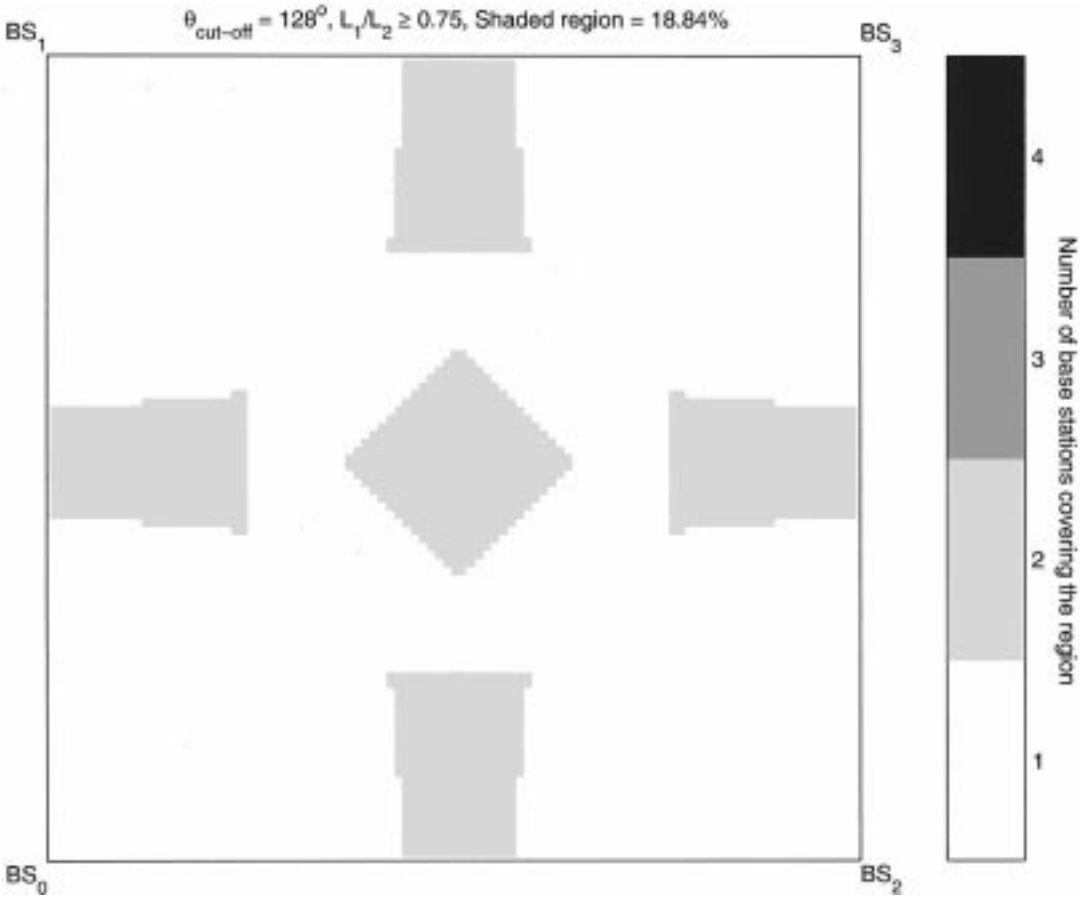

Fig. 11. Areas in a four-sectored rectangular cell that can benefit from cell-site diversity, as predicted by the sinusoidal model with 10% gain reduction allowed.

subscriber terminal. An effort should be made to optimize the subscriber antenna location to obtain a LOS path to each of the hubs.

b) The hubs must be at almost the same distance, with a minimum of 2 km, from the subscriber. The distance ratio between the closer and the farther of the two hubs should not be less than 0.75.

c) The positions of the hubs are such that they make an angle as close as possible to 180° with respect to the subscriber terminal. However, if a slightly reduced diversity gain is allowed, a separation angle as small as 108° is acceptable.

As an example, consider a square area covered by four corner-located base stations, BS_0 through BS_4, which is a part of a larger cellular network with four-sectored rectangular cells. It is assumed that all subscribers in the coverage area satisfy criterion a), whereas both b) and c) are required for the cell-site diversity scheme to work effectively under rainy conditions. It is also assumed that the spacing between two neighboring hubs is 4 km or more, such that subscribers located exactly on the cell border will satisfy criterion b). The portions of the area in which subscriber terminals satisfy these criteria and benefit most from the use of the diversity scheme are illustrated in Fig. 10.

The shaded regions are those that can be covered by two or more base stations under the constraints given above. The total area of these regions is found to be approximately 28% of the nominal service area. It is also observed that these regions are located near the borders among the cells, which are also the locations of subscribers that suffer the most from rain attenuation. Subscribers in areas closer to the base stations, conversely, would not realize much advantage from cell-site diversity but at the same time are less likely to experience outage due to rain attenuation.

When the sinusoidal model, given by expression (6) with $k = 1$, is used, the range of acceptable separation angle becomes 128°–232°. The total area of the regions where cell-site diversity is considered effective predicted by applying the same constraints is found to be around 19% of the nominal service area, as depicted in Fig. 11. This underestimates the portion of service area that can benefit from cell-site diversity, as previously predicted using $k = 0.5$.

When the model with $k = 0.5$ is again used, but this time allowing reduction in diversity gain of as much as 20%, corresponding with $\theta_{\text{cutoff}} = 80°$, the regions that could be effectively covered by more than one hub in a diversity system make up 32% of the nominal service area. As can be seen in Fig. 12, there are even some portions of the area around the center of the square where more than two hubs are available to serve a subscriber station in a diversity configuration.

VI. Summary

Examination of correlations of rain attenuation indicates that correlation between attenuations on two links with angular separations in the range between 100° and 260° is not very sensitive to the angle, which raises an expectation that cell-site diversity under rainy conditions would be equally effective for any

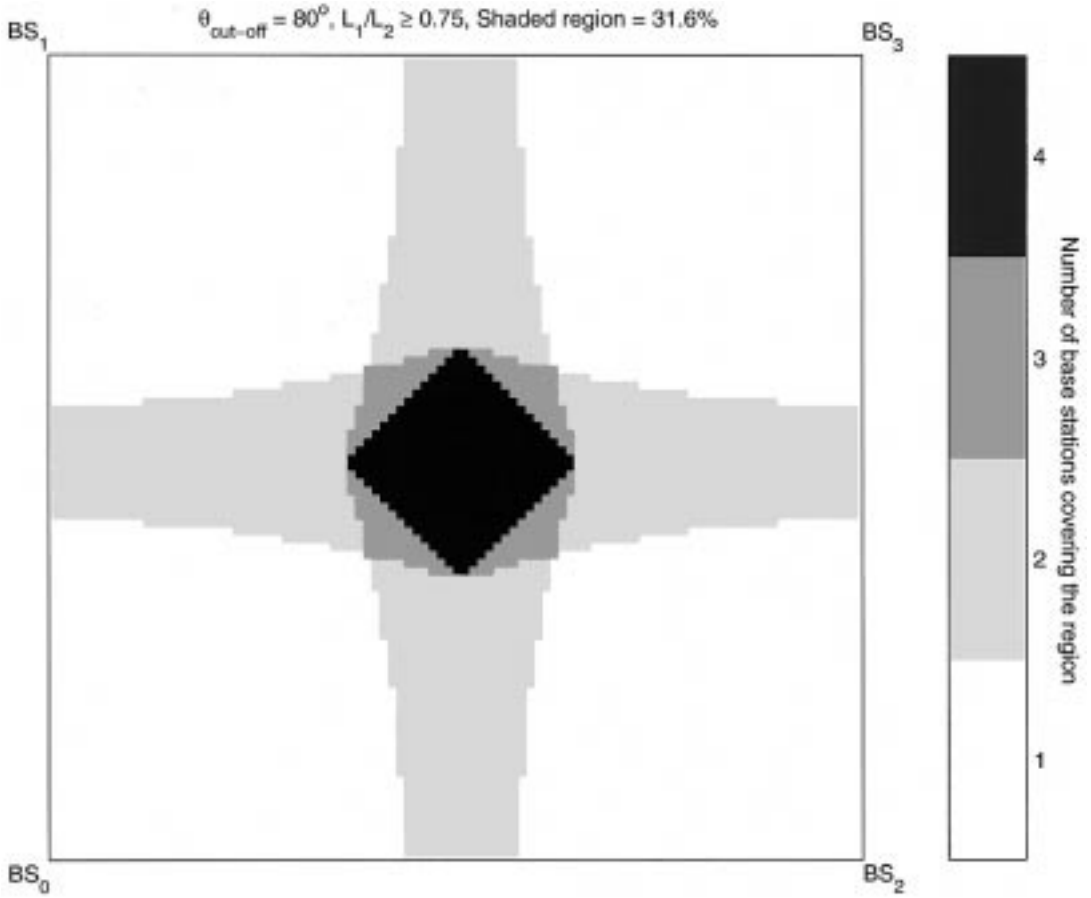

Fig. 12. Areas in a four-sectored rectangular cell that can benefit from cell-site diversity, as predicted by the proposed model with 20% gain reduction allowed.

angular separation within this range. Correlation results for different attenuation (or rain rate) maxima also promise more advantage in the use of cell-site diversity in a heavy storm than in a light rain.

Diversity configurations were simulated for LOS links or links with equal, small obstruction loss assuming selection combining. A profile of diversity gain as a function of separation angle was obtained by fixing one link as the reference and changing the azimuthal orientation of the other link with respect to the convergence point. The shape of the curve, i.e., the symmetry, the maximum gain and the sharpness/flatness around the maximum near 180°, was found to vary from one profile to another, each corresponding to a unique reference link. Accordingly, a new model in the form given by equation (6) was proposed for prediction of diversity gain expected for a combination of link lengths and separation angle at a given time percentage. Two parameters of the model G_{180° and k, each of which varies with link length, angular separation and time percentage, were derived by fitting the model to simulation results obtained for different reference links.

The values of k and sums of squared errors presented in Table I indicate that for arrangements in which the two links are of identical length, a model of root sinusoid can produce better prediction of the variation of diversity gain with angular separation compared to the sinusoidal model in [5]. When the links are different in length, k varies around unity depending on the ratio of the lengths. In this case, a sinusoidal shape can be used to obtain an estimate of the gain variation with respect to separation angle. When the values of G_{180° were examined for links of unequal lengths, it was found that a minimum L_1/L_2 ratio of 0.75, where $L_1 \leq L_2$ are the lengths of the links, is necessary for the diversity system to remain beneficial, at least for 99.9% link reliability and for links ranging from 1 to 4 km.

A set of criteria was suggested for use in assessing the advantages of cell-site diversity for a subscriber station in a fixed cellular system with small cells operating at 30 GHz. When these criteria were applied in a cellular scenario consisting of four-sectored rectangular cells with each square region served by four corner hubs, it was found that 28% of the service area can potentially gain from the application of cell-site diversity under rainy conditions when a reduction in diversity gain of 10% at most is acceptable relative to that for the 180° separation. These regions were found to be concentrated near the borders among the adjacent cells. When a reduction of 20% in diversity gain is allowed, 32% of the service area can benefit from cell-site diversity, with some regions having the possibility of being served by more than two hubs in a diversity mode.

ACKNOWLEDGMENT

The authors would like to thank Dr. I. Zawadzki of the J. S. Marshall Radar Observatory, McGill University, Montreal, QC, Canada, for making the radar measurements and arranging them for use in the work reported herein. The authors also wish to

thank Dr. R. Olsen of the Communications Research Centre for recommending that the work be focused on the spatial variation of rain attenuation, and the use of radar data in simulations, rather than measurements from a few isolated links.

REFERENCES

[1] R. K. Crane, *Electromagnetic Wave Propagation Through Rain*. New York: Wiley, 1996.
[2] W. C. Jakes, *Microwave Mobile Communications*: AT&T IMP Corp., 1994. reprinted by IEEE Press.
[3] H. W. Arnold, D. C. Cox, and R. R. Murray, "Macroscopic diversity performance measured in the 800-MHz portable radio communications environment," *IEEE Trans. Antennas Propagat.*, vol. 36, pp. 277–281, Feb. 1988.
[4] R. L. Freeman, *Radio System Design for Telecommunications*, 2nd ed. New York: Wiley, 1997.
[5] J. Tan and L. Pedersen, "Study of simultaneous coverage and route diversity improvement under rainy periods for LMDS systems at 42 GHz," presented at the ESA Millennium Conf. Antennas and Propagation (AP2000), Davos, Switzerland, Apr. 9–14, 2000.
[6] "Propagation data and prediction methods required for the design of terrestrial broadband millimetric radio access systems operating in a frequency range of about 20–50 GHz," ITU-R, Rec. P.1410, 1999.
[7] G. Hendrantoro, "Estimation of cell area coverage and cell-site diversity gain in 30 GHz fixed cellular systems under rainy conditions," Ph.D. dissertation, Carleton Univ., Ottawa, Canada, 2001.
[8] G. Hendrantoro, D. Falconer, and R. Bultitude, "Preliminary results from the examination of the impact of rain attenuation on EHF cellular radio links," in *Proc. Wireless 2000*, Calgary, Canada, July 10–12, 2000, pp. 146–155.
[9] G. Hendrantoro and I. Zawadzki, "Derivation of Y–Z relation from raindrop size distribution measurements and its application in the calculation of rain attenuation from radar reflectivity factor measurements," *IEEE Trans. Antennas Propagat.*, submitted for publication.
[10] "Specific attenuation model for rain for use in prediction methods," ITU-R, Rec. P.838-1, 1992.
[11] T. Oguchi, "Scattering properties of oblate raindrops and cross polarization of radio waves due to rain: Calculations at 19.3 and 34.8 GHz," *J. Radio Res. Labs.*, vol. 20, no. 102, pp. 79–118, 1973.
[12] G. Seber, *Nonlinear Regression*. New York: Wiley, 1989.

Gamantyo Hendrantoro (M'02) was born on November 11, 1970, in Jombang, Indonesia. He received the B.Eng. (Sarjana) degree in electrical engineering from Institut Teknologi Sepuluh Nopember (ITS) Surabaya, Indonesia, in 1992, and the M.Eng. and Ph.D. degrees in electrical engineering from Carleton University, Ottawa, ON, Canada, in 1997 and 2001, respectively. He also attended a one-term Radar Remote Sensing course at the Atmospheric and Oceanic Sciences, McGill University, Montreal, Canada in 1998.

From 1993 through 1995, he was a Junior Lecturer with the Department of Electrical Engineering, ITS, Indonesia. In 1995, he embarked upon his graduate studies at Carleton University with a Higher Education Project scholarship funding from the Indonesian Ministry of National Education. During his doctoral study, he received the 2000/2001 R.F. Chinnick Memorial Scholarship Award from Telesat Canada and was also one of the recipients of the 2001 Postgraduate Awards for Research Excellence from the Canadian Institute for Telecommunications Research (CITR). Since his graduation in 2001, he has been engaged in a post-doctoral research project at Carleton. His current research interest is in wireless digital communications, with emphasis on radio channel characterization and modeling. He plans to return to Indonesia in 2002 and resume his teaching duties at ITS Surabaya.

Robert J. C. Bultitude (S'74–M'78–SM'00) received the B.Sc. degree in electrical engineering from the University of New Brunswick, Fredericton, NB, Canada, in 1975, and the M.Eng. and Ph.D. degrees in electronics engineering from Carleton University, Ottawa, ON, Canada, in 1979 and 1987, respectively.

His professional career began with Hoyles Niblock Associates in Vancouver, Canada, in 1975, where he worked for two years as a Telecommunications Systems Design Engineer. Then, after receiving the M.Eng. degree, he worked on RF problems in satellite systems with Leigh Instruments, Ottawa. From 1981 to 1989, he was a Telecommunications Research Engineer at CRC. From 1989 to 1996, he was Manager of CRC's Land Mobile and Indoor Radio Propagation (LMIRP) Research Group. In 1996, he relinquished his management role in order to devote more time to research as a Research Scientist studying various propagation and channel modeling issues. His previous research work involves studies on the propagation of UHF radio waves in fresh water and through the water–air interface, analysis and measurement of intermodulation products generated in passive RF components of multifrequency UHF satellite systems, measurement and characterization of fading radio channels, and prediction, based on propagation measurements, of digital error performance on fading channels operating with data rates at which ISI causes significant performance degradation.

Dr. Bultitude was a co-recipient of the IEEE Vehicular Technology Transactions Best Paper of the Year award in 1997, and was a Visiting Scientist at Eindhoven University of Technology, in The Netherlands between Autumn 1998 and Spring 2000. He is a Member of Sigma Xi.

David D. Falconer (M'68–SM'83–F'86) was born in Moose Jaw, SK, Canada on August 15, 1940. He received the B.A.Sc. degree in engineering physics from the University of Toronto, Toronto, ON, Canada, in 1962 and the S.M. and Ph.D. degrees in electrical engineering from Massachusetts Institute of Technology, Cambridge, MA, in 1963 and 1967, respectively.

After a year as a postdoctoral fellow at the Royal Institute of Technology, Stockholm, Sweden he was with Bell Laboratories, Holmdel, NJ, from 1967 to 1980, as a member of the technical staff and later as group supervisor. During 1976–1977, he was a Visiting Professor at Linköping University, Linköping, Sweden. Since 1980, he has been at Carleton University, Ottawa, ON, Canada, where he is a Professor in the Department of Systems and Computer Engineering. His interests are in digital communications and communication theory, with particular application to broadband wireless communications systems. He is currently Director of the Broadband Communications and Wireless Systems Centre (BCWS) at Carleton University. He is active in and has led a broadband wireless research project, involving a number of Canadian universities and companies.

Dr. Falconer was Editor for Digital Communications for the IEEE TRANSACTIONS ON COMMUNICATIONS from 1981 to 1987. He is a member of the Association of Professional Engineers of Ontario. He was awarded the Communications Society Prize Paper Award in Communications Circuits and Techniques in 1983 and again in 1986. He was a co-recipient of the IEEE Vehicular Technology Transactions best paper of the year award in 1992. He is an IEEE Communications Society Distinguished Lecturer.